

1 Development of an all-in-one real-time PCR assay for simultaneous detection of
2 spotted fever group rickettsiae, severe fever with thrombocytopenia syndrome
3 virus and orthohantavirus hantanense prevalent in central China

4 Cuixiang Wang^{1¶}, liangjun Chen^{1¶}, xingrong Li¹, jihong Gu¹, yating Xiang¹, Liang
5 Fang², Lili Chen^{2*} Yirong Li^{1,3,4*}

6 ¹Department of Laboratory Medicine, Zhongnan Hospital of Wuhan University, Wuhan
7 University, Wuhan, China.

8 ²Department of Wuhan EasyDiagnosis Biomedicine, Wuhan, China.

9 ³Wuhan Research Center for Infectious Diseases and Cancer, Chinese Academy of
10 Medical Sciences, Wuhan, People's Republic of China

11 ⁴Hubei Engineering Center for Infectious Disease Prevention, Control and Treatment,
12 Wuhan, People's Republic of China.

13 **These authors contributed equally to this work.**

14 liyirong838@163.com (Y-R L); chenlili@ediagnosis.can (L-L C);

15

16

17

18

19

20

21 **Abstract**

22 Central China has been reported to be one of the most important endemic areas of
23 zoonotic infection by spotted fever group rickettsiae(SFGR), severe fever with
24 thrombocytopenia syndrome virus (SFTSV) and orthohantavirus hantanense(HTNV).
25 Due to similar clinical symptoms, it is challenging to make a definite diagnosis rapidly
26 and accurately in the absence of microbiological tests. In the present study, an all-in-
27 one real-time PCR assay was developed for the simultaneous detection of nucleic acids
28 from SFGR, SFTSV and HTNV. Three linear standard curves for determining SFGR-
29 *ompA*, SFTSV-*L* and HTNV-*L* were obtained within the range of 10^1 - 10^6 copies/ μ L,
30 with the PCR amplification efficiencies ranging from 93.46% to 96.88% and the
31 regression coefficients R^2 of >0.99 . The detection limit was 1.108 copies/ μ L for SFGR-
32 *ompA*, 1.075 copies/ μ L for SFTSV-*L* and 1.006 copies/ μ L for HTNV-*L*, respectively.
33 Both the within-run and within-laboratory coefficients of variation on the cycle
34 threshold (Ct) values were within the range of 0.53%-2.15%. It was also found there
35 was no statistical difference in the Ct values between with and without other non-target
36 bloodborne virus nucleic acids ($P_{\text{SFGR-ompA}}=0.186$, $P_{\text{SFTSV-L}}=0.612$, $P_{\text{HTNV-L}}=0.298$). The
37 sensitivity, specificity, positive and negative predictive value were all 100% for
38 determining SFGR-*ompA* and SFTSV-*L*, 97%, 100%, 100% and 99.6% for HTNV-*L*,
39 respectively. Therefore, the all-in-one real-time PCR assay appears to be a reliable,
40 sensitive, rapid, high-throughput and low cost-effective method to diagnose the

41 zoonotic infection by SFGR, SFTSV and HTNV.

42 **Key Words:** Spotted fever group rickettsiae; Severe fever with thrombocytopenia

43 syndrome virus; Orthohantavirus hantanense; An all-in-one real-time PCR assay;

44 diagnosis

45

46

47

48

49

50

51

52

53

54

55

56

57

58

59

60 **Author Summary**

61 Spotted fever, severe fever with thrombocytopenia syndrome (SFTS), and hemorrhagic
62 fever with renal syndrome (HFERS) sporadically have outbreaks in central China. Due
63 to the similarities in clinical symptoms and the absence of reliable diagnostic methods,
64 clinical diagnosis and treatment frequently result in misdiagnosis or missed diagnosis.
65 Thus, the development of a fast and accurate diagnostic method is crucial for prevention
66 and precise treatment. In this study, we designed an all-in-one real-time PCR assay to
67 differentiate spotted fever group rickettsiae(SFGR), severe fever with
68 thrombocytopenia syndrome virus (SFTSV) and orthohantavirus hantanense(HTNV).
69 The gene *ompA* of SFGR, as well as the gene segment *L* of SFTSV and HTNV, were
70 used as targets to design primers and probes for amplification. Through the verification
71 of nucleic acid and clinical sample detection, the sensitivity of this detection method
72 exceeded 97%, and its specificity was 100%.
73 This new assay could be applied in epidemiology and clinical diagnosis, to control new
74 outbreaks, reduce diagnostic and identification time, and improve test efficiency.

75

76

77

78

79

80 **Introduction**

81 Zoonotic infectious diseases typically occur sporadically and are more prevalent in
82 economically underdeveloped areas, such as remote mountainous and forested regions
83 (1-3). Due to the limited medical laboratory resources and similar clinical symptoms,
84 timely and accurate diagnosis of zoonotic infectious diseases is often difficult, which
85 leads to inadequate and untimely treatment. Since 2009, It has been found that there is
86 a high prevalence of severe fever with thrombocytopenia syndrome (SFTS) in central
87 China including Dabie and Yiling Mountains region(4, 5). SFTS is a zoonotic disease
88 infected by a tick-borne virus called severe fever with thrombocytopenia syndrome
89 virus (SFTSV), a novel *Bandavirus* of family *Phenuiviridae*, which was recently named
90 *Dabie Bandavirus* by The International Committee on Taxonomy of Viruses (ICTV).
91 The main clinical manifestations include acute fever, thrombocytopenia, leukopenia,
92 gastrointestinal and neurological symptoms(6-8), moreover, multiple organ failure may
93 occur in severe cases with a maximum mortality of 30% (9, 10). Recently, tick-borne
94 rickettsioses, another zoonotic infectious disease caused by the spotted fever group
95 rickettsiae (SFGR), was found in succession in central China. SFGR is an intracellular
96 bacteria belonging to the spotted fever group (SFG) of the genus *Rickettsia* in the family
97 *Rickettsiaceae* (11). It was reported that the seroprevalence rate of anti-*Rickettsia*
98 *japonica* antibody is about 21% among people in Yichang, a city in the Yiling
99 Mountains region of central China(12). The main clinical symptoms of tick-borne
100 rickettsioses also include fever and thrombocytopenia as well as headache, muscle pain,

101 rash and local lymphadenopathy(13-16) (12, 17). It is worth noting that central China
102 including the Dabie and Yiling Mountains region is also known to be an important
103 endemic area for orthohantavirus hantanense (HTNV) infections transmitted by rodents,
104 which belongs to the order *Bunyavirales*, family *Hantaviridae*, and
105 genus *Orthohantavirus*(18). The main epidemic strain of HTNV is HV004 in the past
106 ten years(18-20). Hemorrhagic fever with renal syndrome (HFRS), caused by HTNV,
107 is characterized by a combination of symptoms, which include fever, hemorrhage,
108 thrombocytopenia and acute kidney injury (21, 22). The early clinical manifestations
109 of these pathogens infections are often similar and nonspecific, with most patients
110 experiencing systemic symptoms such as fever, thrombocytopenia, headache, fatigue
111 and muscle aches (23, 24). Therefore, it is challenging to rapidly and accurately identify
112 these pathogens in febrile patients with thrombocytopenia and a history of outdoor
113 activities in central China.

114 There are a variety of methods including antigen-antibody detection and nucleic acid
115 testing to be used for the identification of microbial pathogens. Antigen-antibody
116 detection such as Enzyme-linked immunosorbent assay and indirect
117 immunofluorescence are limited in the precise diagnosis due to wide antigen cross-
118 reactivity and delayed seroconversion (25-27). Nucleic acid testing has always been
119 considered to be the preferred method for diagnosing viral infections, including
120 quantitative real-time fluorescence PCR assay, isothermal amplification reaction,

121 digital PCR assay and metagenomics next generation sequencing (mNGS). Although
122 isothermal amplification reactions is rapid and do not require a specialized
123 thermocycler, it have high requirements for primer designing and serious challenges for
124 a multiplex PCR assay. Digital PCR assay and mNGS have their advantages in absolute
125 quantification and unbiased microbial infection, respectively, but it is not unsuitable to
126 carry out in hospitals located in economically underdeveloped remote areas due to their
127 high cost or time-consuming procedure. It has been reported that the real-time PCR
128 assay is the preferred choice for detecting the nucleic acid of viruses due to its high
129 accuracy, faster testing time and lower cost. It was also found that there was only one
130 commercially available kit for testing target nucleic acids of SFTSV. Therefore, in
131 order to quickly diagnose these zoonotic infectious diseases caused by SFGR, SFTSV
132 and HTNV in central China, we established a rapid, convenient and accurate all-in-one
133 real-time PCR assay following the evaluation of clinical performances.

134

135

136

137

138

139 **Materials and methods**

140 **Serum or nucleic acid samples**

141 A total of 325 serum or nucleic acid samples were collected in present study. Of them,
142 17 SFGR DNA-positive nucleic acid samples were obtained from Beijing Center For
143 Disease Control And Prevention (CDC) (n=9) and State Key Laboratory of Virology
144 (n=8), 33 HTNV RNA-positive nucleic acid samples were prepared in State Key
145 Laboratory of Virology (n=21) and Hubei CDC(n=12), the remaining including 46
146 SFTSV RNA-positive nucleic acid samples and 229 serum samples without three target
147 pathogens were garnered from Zhongnan Hospital of Wuhan University. These nucleic
148 acid samples were previously tested to be positive for SFTSV, Hepatitis B virus (HBV),
149 hepatitis C virus (HCV), Epstein-Barr virus (EBV) and cytomegalovirus (CMV) by
150 commercially available kits (DaAn Gene Co., Ltd), for SFGR DNA and HTNV RNA
151 by Sanger sequencing after nested PCR, respectively(12, 18). The study was approved
152 by the Ethics Committee of Zhongnan Hospital of Wuhan University.

153 **Primers and probes**

154 All primers and probes were synthesized by General Biosystems (Anhui, China). The
155 detailed primers and probes sequences are listed in **Table 1**. The primers ompA-F/R,
156 and the probe ompA-P were used to amplify the target gene *ompA* in the SFGR. The 5'-
157 ends and 3'-ends of ompA-P were labeled with FAM (6-carboxyfluorescein) and Black
158 Hole Quencher 1 (BHQ1), respectively. The primer pair DL-F/R, and the probe DL-P
159 were employed to amplify the gene segment *L* in SFTSV. The VIC(5-VIC
160 phosphoramidite) and Black Hole Quencher 2 (BHQ2) were labeled in the 5'-ends and

161 3'-ends of DL-P, respectively. Two sets of primers and probes including HL-F1/R1 and
162 HL-P1, and HL-F2/R2 and HL-P2, were simultaneously adopted to amplify the gene
163 segment *L* in HTNV, and both the 5'-ends and 3'-ends of HL-P1 as well as HL-P2 were
164 labeled with Cy5 (Cyanine 5) and BHQ2, respectively. *Beta-actin* (*ACTB*) was used as
165 the endogenous reference gene in the all-in-one real-time PCR assay. ACTB-F1,
166 ACTB-R1 and ACTB-P were employed to amplify *ACTB*, and the 5'-ends and 3'-ends
167 of ACTB-P were labeled with 5-Carboxy-X-rhodamine (ROX) and BHQ2. All of the
168 primers and probes for amplifying *ompA* and *L* were designed using PrimerPrimer 5.0
169 design software, whereas those for amplifying the *ACTB* were the same as those used
170 in previous studies (28). (**Scheme 1**).

171

172

173

174

175

176

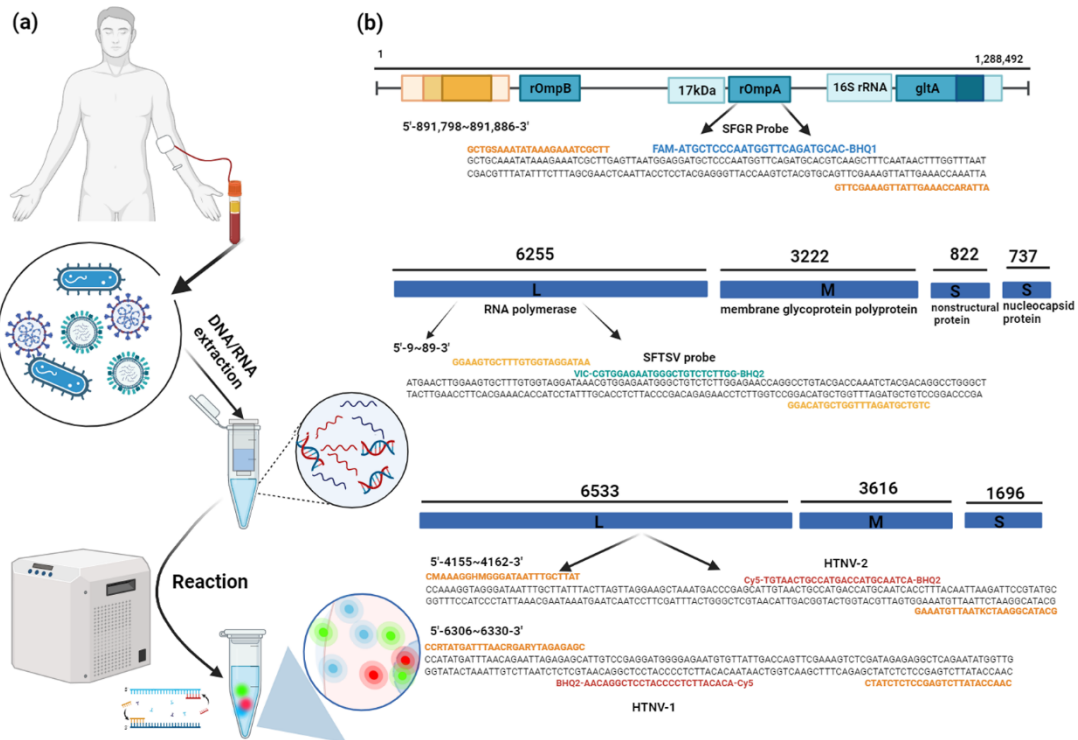
177

178

179 **Table 1. Primers and probes used in the all-in-one real-time PCR assay.**

180 a:AE006914.1; b:NC_043450.1;c:NC_005222.1; d:JQ083393.1; e:KR710455.1.

pathogen	Primers and probes	Nucleotide sequence (5'-3')	Gene or segments	Position	Product length (bp)
SFGR	OmpA-probe	FAM- ATGCTCCCAATGGTTCAGATGCAC- BHQ1	<i>OmpA</i>	1176385	89
	OmpA-F	GCTGSAAATATAAAGAAATCGCTT		-	
	OmpA-R	ATTARACCAAAGTTATTGAAAGCTTG		1176473 ^a	
SFTSV	DL-probe	VIC- CGTGGAGAATGGGCTGTCTCTTGG- BHQ2	<i>L</i>	9-89 ^b	81
	DL-F	GGAAGTGCTTTGTGGTAGGATAA			
	DL-R	CTRTCGTAGATTTGGTCRTACAGG			
HTNV	HL-probe1	Cy5- ACACATTCTCCCCATCCTCGGACAA- BHQ2	<i>L</i>	6278- 6377 ^c	100
	HL-F1	CCRTATGATTTAACRGARYTAGAGA GC			
	HL-R1	CAACCATAYTYTGAGCCTCTCTATC			
	HL-probe2	Cy5- TGTAAGTCCATGACCATGCAATCA- BHQ2		4155- 4262 ^d	
	HL-F2	CMAAAGGHMGGGATAATTTGCTTAT			
	HL-R2	GCATACGGAATCKTAATTGTAAAG			
ACTB	ACTB-probe	ROX-ACCACCACGGCCGAGCGG- BHQ2	<i>ACTB</i>	648-706 ^e	59
ACTB-F	GAGCGCGGCTACAGCTT				
ACTB-R	TCCTTAATGTCACGCACGATTT				



181

182 **Scheme 1. Schematic illustration of the proposed all-in-one real-time PCR assay**

183 (a) Detection principle schematic diagram;(b) Schematic of the SFGR, SFTSV or

184 HTNV genome and corresponding primer sequence design.

185

186 DNA/RNA extraction

187 DNA and RNA were extracted according to the instructions of the Vazyme Fast Pure

188 Viral DNA/RNA Mini Kit Pro (Vazyme Biotech Co.,Ltd). All of the nucleic acid

189 samples used in the present study were stored at -80 °C until further experiments.

190

191 Construction of the plasmids

192 Plasmids SFGR-*ompA*, SFTSV-*L*, HTNV-*L1* and HTNV-*L2* constructed by General
193 Biol (Anhui) Co., Ltd were used to create standard curves and determine the limit of
194 detection (LOD) for the all-in-one real-time PCR assay. The copy number of plasmid
195 was calculated using the formula: plasmid copy number (copies/ μ L) = plasmid
196 concentration $\times 10^{-9} \times$ diluted multiples $\times 6.02 \times 10^{23}$ / (660 Dalton/bases \times DNA
197 length in nucleotides). The initial concentrations of these plasmids were determined to
198 be 6.92×10^9 copies/ μ L for SFGR-*ompA*, 5.30×10^9 copies/ μ L for SFTSV-*L*, $6.80 \times$
199 10^9 for HTNV-*L1* and 5.79×10^9 copies/ μ L for HTNV-*L2*, respectively. All of them
200 were stored at -80°C for future experiments.

201

202 **All-in-one real-time PCR assay**

203 The all-in-one real-time PCR assay was carried out in an Eppendorf tube for the
204 simultaneous detection of gene *ompA* in the SFGR, segment *L* in both SFTSV and
205 HTNV, and the house-keeping gene *ACTB* with a Gentier 96E/96R real-time
206 thermocycler (Tianlong, Xi'an, China). The final volume of the all-in-one real-time
207 PCR was $25\mu\text{L}$, comprising $5.0\mu\text{L}$ of $5\times$ Neoscript Fast RT Premix Buffer, $1.0\mu\text{L}$ of
208 $25\times$ Neoscript Fast RTase/UNG Mix, $0.5\mu\text{L}$ of an *ompA*-F and *ompA*-R
209 mixture(300pmol/mL), $0.5\mu\text{L}$ of a DL-F and DL-R mixture(200pmol/mL), $0.5\mu\text{L}$ of an
210 HL-F1 and HL-R1 mixture(600pmol/mL), $0.5\mu\text{L}$ of an HL-F2 and HL-R2
211 mixture(600pmol/mL), $0.5\mu\text{L}$ of an *ACTB* forward and reverse primers mixture. $1\mu\text{L}$

212 each of ompA-P, DL-P, HL-P1, HL-P2 and ACTB probes (100pmol/mL), 2 μ L of
213 template and 9.5 μ L of ddH₂O. The optimized thermal cycling conditions for
214 amplification were as follows: 1 cycle of reverse transcription at 50°C for 15 minutes
215 and pre-denaturation at 95°C for 3 minutes, followed by 45 cycles of denaturation at 95°C
216 for 10 seconds and annealing/ extension at 60°C for 30 seconds. Monitoring of
217 fluorescence occurred at the extension phase. The Cycle threshold (Ct) values obtained
218 from the all-in-one real-time PCR assay were adopted for the discrimination of the
219 presence of the target gene in clinical samples or not.

220

221 **Evaluation of PCR efficiency, LOD and precision of the all-** 222 **in-one real-time PCR assay**

223 The amplification efficiency of the all-in-one real-time PCR assay was deduced from
224 standard curves as described previously(29), which were generated by plotting the Ct
225 values versus the log₁₀ DNA concentration of the standards followed by constructing a
226 linear regression equation. To construct the standard curve, six 10-fold dilutions of the
227 plasmids SFGR-*ompA*, SFTSV-*L*, and HTNV-*L2* starting with $\sim 10^6$ copies/ μ L and
228 ending with $\sim 10^1$ copies/ μ L, were yielded, respectively.

229 LOD was determined according to Chinese National Standard GB/T 37871-2019(30).

230 In brief, plasmids standards at $\sim 10^1$ copies/ μ L were absolutely quantified using a digital

231 PCR assay, then were serially two-fold diluted to be about 1 copies/ μ L. Each diluted

232 plasmid was run in 20 replicates to determine the LOD of the all-in-one real-time PCR
233 assay.

234 The precision of the all-in-one real-time PCR assay was evaluated according to EP15-
235 A2 (31). In brief, the evaluation was performed per day with three replicate samples at
236 each of two concentrations ($\sim 10^4$ and $\sim 10^0$ copies/ μL) daily for five days. Imprecision
237 was assessed by using the coefficient of variation (CV) on the Ct values.

238

239 **Analysis of specificity and interference**

240 A total of 4 nucleic acid samples from other bloodborne viruses were adopted to analyze
241 specificity. Then they were separately tested using the all-in-one real-time PCR assay
242 to investigate nonspecific amplification. In addition, single or multiple target nucleic
243 acids at a concentration of LOD were performed on the all-in-one real-time PCR assay
244 without or with these nucleic acids from other bloodborne viruses in three replicates,
245 then the statistical difference was calculated by an independent samples *t*-test on the Ct
246 values to evaluate interference from HBV, HCV, EBV and CMV nucleic acids.

247

248 **Evaluation of the accuracy of the all-in-one real-time PCR** 249 **assay**

250 To evaluate of accuracy of the all-in-one real-time PCR assay, 321 nucleic acid samples
251 were tested. The results were compared to those reported previously. Sensitivity,

252 specificity, positive and negative predictive values (PPV and NPV) were calculated .

253

254

255

256

257

258

259

260

261

262

263

264

265

266

267

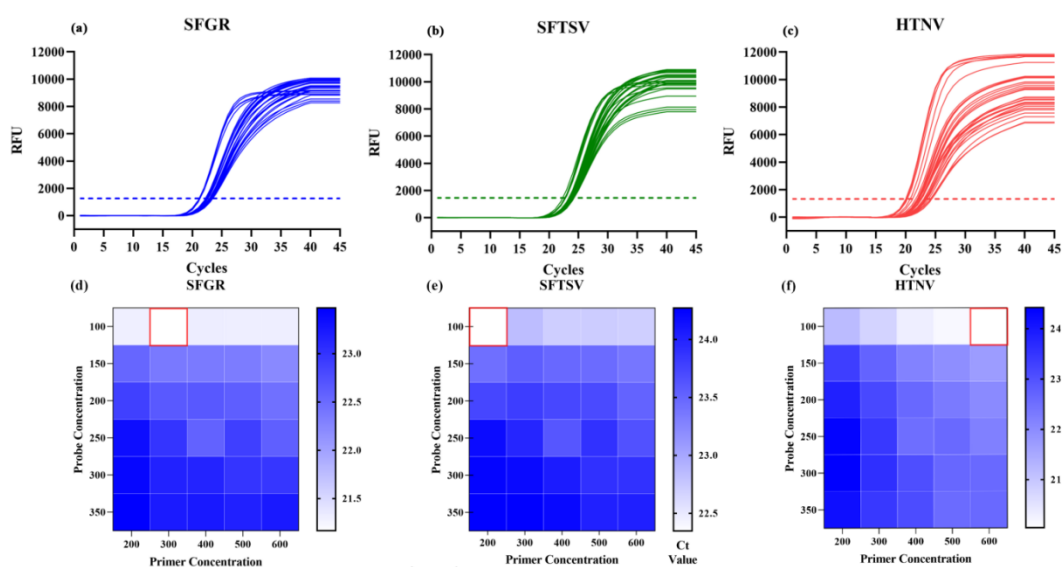
268

269

270 **Results**

271 **Optimal conditions for the all-in-one real-time PCR assay**

272 Our experimental data indicated that the optimal annealing/extension temperature was
273 60°C (Table S1). In addition, to ensure the optimal conditions for detection, the
274 concentrations of primers and probes for amplifying the target gene or gene fragments
275 of SFGR, SFTSV and HTNV were elaboratively optimized. As seen in Fig 1, the
276 optimal concentration of primers ompA-F/R, DL-F/R, HL-F1/R1 and HL-F2/R2 is
277 300pmol/mL, 200pmol/mL, 600pmol/mL and 600pmol/mL, respectively. While the
278 optimal concentration of all probes is 100pmol/mL. It was shown that when the all-in-
279 one real-time PCR assay had primers and probes at the optimal concentrations, the
280 lowest Ct values were yielded (Table S2-S4).

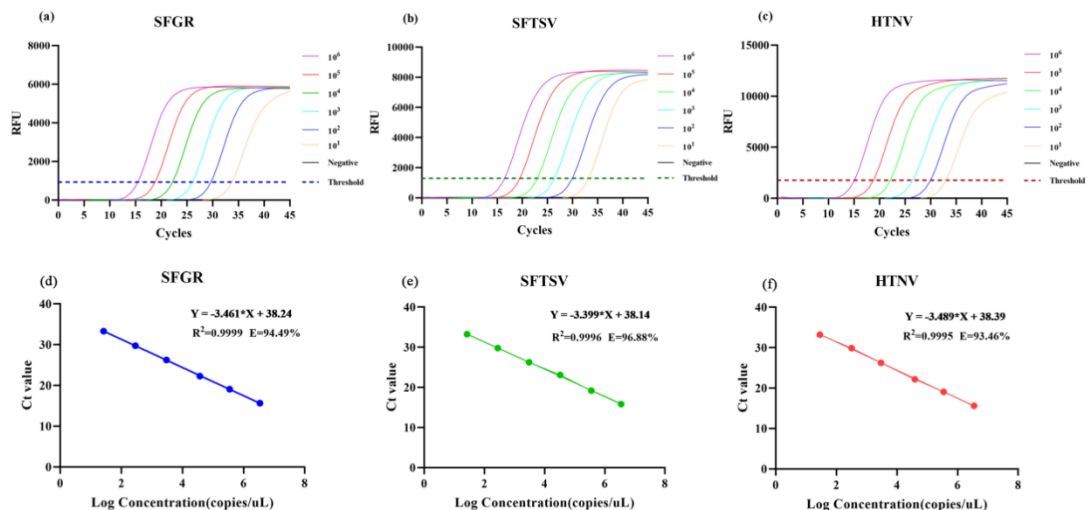


281
282 **Fig 1. Primer and probe concentration optimization.** (a) SFGR's amplification curve;
283 (b)SFTSV's amplification curve; (c)HTNV's amplification curve;(d) SFGR best primer
284 concentration 300pmol/mL, best probe concentration 200pmol/mL; (e) SFTSV best
285 primer concentration 200pmol/mL, best probe concentration 100pmol/mL;(f) HTNV

286 best primer concentration 600pmol/mL, best probe concentration 100pmol/mL

287 PCR efficiency, LOD and precision of all-in-one real-time 288 PCR assay

289 Serial dilutions of four plasmids were co-amplified using the all-in-one real-time PCR
290 assay to construct standard curves. Three linear standard curves were obtained within
291 the range of 10^1 - 10^6 copies/ μ L with regression coefficients R^2 ranging from 0.9995 to
292 0.9999, and amplification efficiencies ranging from 93.46% to 96.88% (Fig 2). The
293 LOD were determined to be 1.108 copies/ μ L for the SFGR-*ompA*, 1.075 copies/ μ L for
294 the SFTSV-*L* and 1.006 copies/ μ L for the HTNV-*L* with a detection rate of more than
295 95%. Regardless of target nucleic acids, the within-run CVs ranged from 0.53%~1.99%,
296 whereas the within-laboratory CVs were limited to the range between 0.79% and 2.15%.
297 (Table 2)



298

299 Fig 2. Amplification curves and standard curve construction used about 10^6 ~ 10^1

300 **copies/μL plasmids.** (a) SFGR's amplification curve; (b)SFTSV's amplification curve;
 301 (c)HTNV's amplification curve; (d) SFGR's standard curve; (e)SFTSV's standard curve;
 302 (f)HTNV's standard curve; The all-in-one real-time PCR assay reaction is performed
 303 using the optimal primer concentration. 95°C for 3 minutes; denaturation at 95°C for 10
 304 seconds; annealing/elongation at 60°C for 30 seconds. 45 cycles.

305

306

307

308

309

310

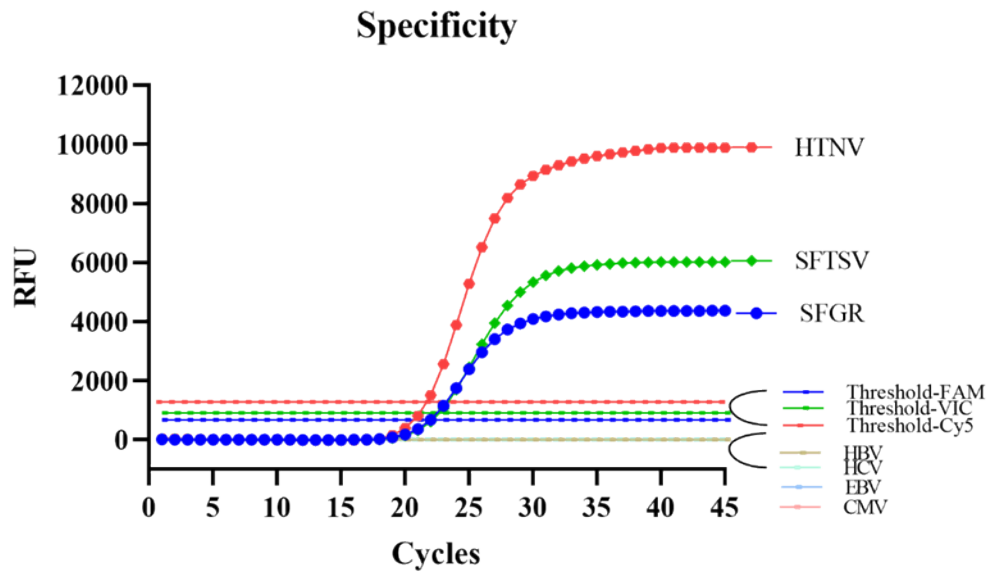
311 **Table 2. Within-run and within-laboratory reproducibility of the all-in-one real-**
 312 **time PCR assay.**

Pathogen	Standard concentration (copies/μL)	Within-run			Within-laboratory		
		Mean Ct	SD	CV(%)	Mean Ct	SD	CV(%)
SFGR- <i>ompA</i>	32,629.9	20.46200	0.10752	0.53%	20.61280	0.16201	0.79%
	2.217	34.87633	0.35874	1.03%	35.17633	0.63580	1.81%
SFTSV- <i>L</i>	36,294.4	21.95167	0.20802	0.95%	21.83000	0.30018	1.38%
	2.151	35.80333	0.55486	1.55%	35.45907	0.68253	1.92%
HTNV- <i>L</i>	35,303.3	20.41267	0.14856	0.73%	20.99873	0.38912	1.85%
	2.013	34.00400	0.67554	1.99%	33.94393	1.11306	2.15%

313 SFGR: spotted fever group rickettsiae; SFTSV: severe fever with thrombocytopenia
314 syndrome virus; HTNV: orthohantavirus hantanense.

315 **Specificity and the anti-interference ability of the all-in-one** 316 **real-time PCR assay**

317 Four nucleic acid samples which were previously tested positive for HBV-DNA, HCV-
318 RNA, EBV-DNA and CMV-DNA, respectively, were performed to evaluate the
319 specificity of the all-in-one real-time PCR assay. All of them yielded horizontal
320 amplification plots, whereas only plasmids SFGR-*ompA*, SFTSV-*L*, and HTNV-*L*
321 yielded classical “S” type curves (**Fig 3**). Then the plasmids were tested to evaluate the
322 interference from HBV-DNA, HCV-RNA, EBV-DNA and CMV-DNA. The resulting
323 Ct values are listed in Table 3. It was found there was no statistical difference in the Ct
324 values between single fluorescence and multiple fluorescence assays for all three targets
325 ($P_{\text{SFGR}}=0.186$, $P_{\text{SFTSV}}=0.612$, $P_{\text{HTNV}}=0.298$). It was also shown that the Ct value
326 fluctuation was less than 1.1 when the non-target bloodborne virus nucleic acids were
327 added (**Table 3**).



328

329 **Fig 3. Results of specificity experiment.** Only the positive control well has an
 330 amplification curve; HBV, HCV, EBV and CMV show no reaction curves.

331 **Table 3. The Ct values variation after adding non-specific nucleic acids.**

pathogens		Ct values						
		HBV	HCV	EBV	CMV	HBV	HCV	EBV
Single template	SFGR- <i>ompA</i>	34.996	35.262	35.066	34.965	35.707	35.207	35.574
	SFTSV- <i>L</i>	36.926	36.645	36.520	35.918	36.121	36.121	35.887
	HTNV- <i>L</i>	35.621	35.793	35.652	36.355	36.059	36.309	35.941
Multiple template ^a	SFGR- <i>ompA</i>	35.316	35.496	35.137	35.723	35.699	36.160	35.988
	SFTSV- <i>L</i>	36.707	36.707	36.426	35.730	35.527	36.387	35.910
	HTNV- <i>L</i>	35.301	35.598	35.699	36.027	36.293	35.590	36.395

332 ^aMultiple template: SFGR, SFTSV and HTNV mixed as a template (SFGR:1.108
 333 copies/ μ L; SFTSV:1.075 copies/ μ L; HTNV:1.006 copies/ μ L).

334 **Evaluation accuracy of all-in-one real-time PCR assay with**
 335 **clinical samples**

336 Judgment criteria are as follows: (a) Positive: Ct<37 and a typical amplification curve

337 is observed ($Ct_{ACTB}22.48-27.67$). (b) Negative: no Ct value and no amplification
338 curve($Ct_{ACTB}22.48-27.67$). (c) Retesting: $Ct > 37$ and a typical amplification curve is
339 observed. If the retest result is the same as mentioned above, it is considered positive;
340 otherwise, it is deemed negative($Ct_{ACTB}22.48-27.67$). (d) Unqualified DNA sample:
341 $Ct_{ACTB} < 22.48$ and $Ct_{ACTB} > 27.67$ (Ct_{ACTB} were calculated from the Ct values of 321
342 characterized samples with mean and standard deviation (SD): 25.07 ± 2.60).

343 A total of 321 samples were collected to evaluate the accuracy of the all-in-one real-
344 time PCR assay. It was found the sensitivity, specificity, positive and negative
345 predictive value for testing SFGR-*ompA* and SFTSV-*L* nucleic acids were all 100%,
346 whereas the detection of HTNV-*L* was 97%, 100%, 100% and 99.6%, respectively.

347 (Table 4)

348

349

350

351

352

353

354 **Table 4. The sensitivity, specificity, PPV and NPV of the all-in-one real-time PCR**
355 **assay.**

pathogen	Outcome	Control method	All-in-one real-time PCR assay	Sensitivity	Specificity	PPV ^a	NPV ^b
SFGR-<i>ompA</i>	Positive	17	17	100%	100%	100%	100%
	Negative	225	225				
SFTSV-<i>L</i>	Positive	46	46	100%	100%	100%	100%
	Negative	225	225				
HTNV-<i>L</i>	Positive	33	32	97%	100%	100%	99.6%
	Negative	225	225				

356 ^aPPV: Positive Predictive Value; ^bNPV: Negative Predictive Value.

357

358

359

360

361

362

363

364

365

366

367

368

369 **Discussion**

370 In the present study, an all-in-one real-time PCR was successfully established to

371 simultaneously detect the nucleic acids from SFGR, SFTSV and HTNV. The SFGR-
372 *ompA*, as well as the gene segment *L* of SFTSV and HTNV, were used as targets for
373 amplification. It was worth noting that two sets of primer and probe were used to
374 amplify gene segment *L* of HTNV due to high variation in China(32). China has had
375 the highest number of HFRS cases worldwide. There exist numerous branches of
376 HTNV, with highly diverse genetics in Heilongjiang, Shanxi, Liaoning, Shandong, Jilin,
377 Hebei, Hunan, Zhejiang, Jiangxi, Jiangsu and Hubei provinces(33). Recently, the
378 genetic evolution analysis of the *L* segment revealed that the viral sequences prevalent
379 in Hubei province cluster together, forming a distinct lineage with genetic variations
380 from viruses in other regions(18). To enhance our detection capabilities, we have
381 designed two sets of primer and probe for HTNV infection. HTNV-*L2* is primarily
382 utilized to detect the unique lineage (HV004-like) that is prevalent in Hubei province,
383 whereas HTNV-*L1* is employed for detecting infection in other regions.

384 The all-in-one real-time PCR method demonstrated high sensitivity, with the ability to
385 detect approximately 1000 copies/ml of the virus genome. It also exhibited an excellent
386 linear range between 10^6 and 10^1 copies/ μ L, where the regression coefficients R^2 for
387 the target nucleic acids ranged from 0.9995 to 0.9999 and the PCR amplification
388 efficiencies ranged from 93.46% to 96.88%, with a dynamic range of six orders of
389 magnitude (10^1 - 10^6 copies/ μ L). To assess its specificity, we confirmed that other
390 related viruses such as HBV, HCV, EBV and CMV did not produce positive signals

391 and did not affect the Ct value of the positive target, indicating the high specificity of
392 the detection method. Furthermore, the detection method showed high reproducibility,
393 with relatively small variations observed in both intra-assay and inter-assay capabilities.
394 The average coefficients of variation (CVs) for within-run and within-laboratory was
395 limited to the range between 0.53%-2.15%, which is considered acceptable in terms of
396 reproducibility. Using the all-in-one real-time PCR method, we successfully detected
397 SFGR, SFTSV and HTNV in 321 expected clinical samples. Among these samples, 17
398 were identified as SFGR positive, 46 as SFTSV positive and 33 as HTNV positive. The
399 detection system's sensitivity, specificity, PPV and NPV for SFGR and SFTSV were
400 all 100%, while the detection of HTNV was 97%, 100%, 100% and 99.6%. These
401 results demonstrate the effectiveness of the all-in-one real-time PCR assay in detecting
402 and differentiating these pathogens in clinical samples.

403 Since zoonotic infectious diseases like SFTSV, HTNV and SFGR are often prevalent
404 in economically underdeveloped areas, the risk of misdiagnosis is high due to their
405 similar clinical symptoms. Therefore, it is crucial to develop and evaluate a multiplex
406 assay that can detect and identify these similar pathogens simultaneously. So far, there
407 only exists single real-time fluorescence PCR detection methods for SFTSV and HTNV.
408 In comparison, our all-in-one real-time PCR method can simultaneously detect SFGR,
409 SFTSV, and HTNV, making it advantageous for identifying and detecting similar
410 symptoms in patients, as well as conducting large-scale screenings in epidemic

411 areas(34-36). In comparison to the immunochromatographic assay (ICA), which is a
412 cheaper and more convenient on-site testing method but has limitations in terms of
413 sensitivity and delayed detection windows, our method offers a longer detection
414 window and higher sensitivity(37). Compared to the SFTSV CRISPR detection method
415 established by Zou et al., our detection method offers lower detection limits (about 1
416 copy/ μ L), reduced costs, and the ability to conduct multiple detections. However, it
417 should be noted that our method has a slightly longer detection time of 60 minutes when
418 compared to their CRISPR detection method(38, 39). For other methods, such as virus
419 isolation, a long experimental cycle of about 10 to 15 days is required in comparison
420 with PCR, thus rendering them unsuitable for clinical promotion. Metagenomic
421 sequencing offers the advantage of detecting a wide range of pathogens without bias
422 and conducting systematic geographical analysis, but its lack of standardization, limited
423 personnel expertise, and high cost hinder its widespread application in clinical
424 practice(40). Overall, the all-in-one real-time PCR assay we have established has the
425 advantages of lower detection limits, lower costs, shorter processing time, and longer
426 detection window period, making it suitable for application in primary medical
427 institutions and remote areas.

428 Our research demonstrates that all-in-one real-time PCR assay testing has high
429 sensitivity, specificity and reproducibility. Additionally, the turnaround time for
430 experiments is approximately 2 hours, including nucleic acid extraction steps. This

431 makes it a high-throughput, reliable and cost-effective diagnostic and screening tool for
432 early clinical diagnosis of acute-phase SFTSV, HTNV and SFGR. Consequently, the
433 all-in-one real-time PCR assay enables the simultaneous detection of multiple
434 pathogens in a single reaction system, offering great potential for future clinical point-
435 of-care applications. This advancement holds promise in assisting with early and
436 accurate diagnosis, as well as contributing to effective public health management and
437 infectious disease control.

438 **Acknowledgments**

439 We are grateful to the Beijing Center For Disease Control And Prevention and State
440 Key Laboratory of Virology for providing experimental facilities.

441

442

443

444

445

446

447

448

449 Uncategorized References

- 450 1. Han BA, Kramer AM, Drake JM. Global Patterns of Zoonotic Disease in Mammals. Trends
451 in Parasitology. 2016;32(7):565-77.
- 452 2. Plowright RK, Parrish CR, McCallum H, Hudson PJ, Ko AI, Graham AL, et al. Pathways to
453 zoonotic spillover. Nature Reviews Microbiology. 2017;15(8):502-10.
- 454 3. Tomori O, Oluwayelu DO. Domestic Animals as Potential Reservoirs of Zoonotic Viral
455 Diseases. Annual Review of Animal Biosciences. 2023;11:33-55.
- 456 4. Zhang YZ, He YW, Dai YA, Xiong Y, Zheng H, Zhou DJ, et al. Hemorrhagic fever caused
457 by a novel Bunyavirus in China: pathogenesis and correlates of fatal outcome. Clin Infect Dis.
458 2012;54(4):527-33.
- 459 5. Ren YT, Tian HP, Xu JL, Liu MQ, Cai K, Chen SL, et al. Extensive genetic diversity of
460 severe fever with thrombocytopenia syndrome virus circulating in Hubei Province, China, 2018-
461 2022. PLoS Negl Trop Dis. 2023;17(9):e0011654.
- 462 6. Zhuang L, Sun Y, Cui XM, Tang F, Hu JG, Wang LY, et al. Transmission of Severe Fever
463 with Thrombocytopenia Syndrome Virus by Haemaphysalis longicornis Ticks, China. Emerg
464 Infect Dis. 2018;24(5):868-71.
- 465 7. Wang M, Huang P, Liu W, Tan W, Chen T, Zeng T, et al. Risk factors of severe fever with
466 thrombocytopenia syndrome combined with central neurological complications: A five-year
467 retrospective case-control study. Front Microbiol. 2022;13:1033946.
- 468 8. Li DX. Severe fever with thrombocytopenia syndrome: a newly discovered emerging
469 infectious disease. Clin Microbiol Infect. 2015;21(7):614-20.

- 470 9. Li J, Li S, Yang L, Cao P, Lu J. Severe fever with thrombocytopenia syndrome virus: a
471 highly lethal bunyavirus. *Crit Rev Microbiol*. 2021;47(1):112-25.
- 472 10. Yu XJ, Liang MF, Zhang SY, Liu Y, Li JD, Sun YL, et al. Fever with thrombocytopenia
473 associated with a novel bunyavirus in China. *N Engl J Med*. 2011;364(16):1523-32.
- 474 11. Parola P, Paddock CD, Raoult D. Tick-borne rickettsioses around the world: emerging
475 diseases challenging old concepts. *Clin Microbiol Rev*. 2005;18(4):719-56.
- 476 12. Teng Z, Gong P, Wang W, Zhao N, Jin X, Sun X, et al. Clinical Forms of Japanese Spotted
477 Fever from Case-Series Study, Zigui County, Hubei Province, China, 2021. *Emerg Infect Dis*.
478 2023;29(1):202-6.
- 479 13. Efstratiou A, Karanis G, Karanis P. Tick-Borne Pathogens and Diseases in Greece.
480 *Microorganisms*. 2021;9(8).
- 481 14. Noguchi M, Oshita S, Yamazoe N, Miyazaki M, Takemura YC. Important Clinical Features
482 of Japanese Spotted Fever. *Am J Trop Med Hyg*. 2018;99(2):466-9.
- 483 15. Parola P, Davoust B, Raoult D. Tick- and flea-borne rickettsial emerging zoonoses. *Vet*
484 *Res*. 2005;36(3):469-92.
- 485 16. Helmick CG, Bernard KW, D'Angelo LJ. Rocky Mountain spotted fever: clinical, laboratory,
486 and epidemiological features of 262 cases. *J Infect Dis*. 1984;150(4):480-8.
- 487 17. Li W, Liu SN. *Rickettsia japonica* infections in Huanggang, China, in 2021. *IDCases*.
488 2021;26:e01309.
- 489 18. Chen JT, Zhan JB, Zhu MC, Li KJ, Liu MQ, Hu B, et al. Diversity and genetic

- 490 characterization of orthohantavirus from small mammals and humans during 2012-2022 in
491 Hubei Province, Central China. *Acta Trop.* 2023;249:107046.
- 492 19. Li JL, Ling JX, Liu DY, Liu J, Liu YY, Wei F, et al. Genetic characterization of a new subtype
493 of Hantaan virus isolated from a hemorrhagic fever with renal syndrome (HFRS) epidemic area
494 in Hubei Province, China. *Arch Virol.* 2012;157(10):1981-7.
- 495 20. Brocato RL, Hooper JW. Progress on the Prevention and Treatment of Hantavirus Disease.
496 *Viruses.* 2019;11(7).
- 497 21. Jonsson CB, Figueiredo LT, Vapalahti O. A global perspective on hantavirus ecology,
498 epidemiology, and disease. *Clin Microbiol Rev.* 2010;23(2):412-41.
- 499 22. Wang ML, Wang JP, Wang TP, Li J, Hui L, Ha XQ. Thrombocytopenia as a Predictor of
500 Severe Acute Kidney Injury in Patients with Hantaan Virus Infections. *Plos One.* 2013;8(1).
- 501 23. Zhao B, Hou HH, Gao R, Tian B, Deng BC. Mononucleosis-like illnesses due to co-
502 infection with severe fever with thrombocytopenia syndrome virus and spotted fever group
503 rickettsia:a case report. *Bmc Infectious Diseases.* 2021;21(1).
- 504 24. Zhan JB, Cheng J, Hu B, Li J, Pan RG, Yang ZH, et al. Pathogens and epidemiologic
505 feature of severe fever with thrombocytopenia syndrome in Hubei province, China. *Virus*
506 *Research.* 2017;232:63-8.
- 507 25. Lee K, Choi MJ, Cho MH, Choi DO, Bhoo SH. Antibody production and characterization of
508 the nucleoprotein of severe fever with thrombocytopenia syndrome virus (SFTSV) for effective
509 diagnosis of SFTSV. *Virol J.* 2023;20(1):206.

- 510 26. Noden BH, Tshavuka FI, van der Colf BE, Chipare I, Wilkinson R. Exposure and risk
511 factors to *coxiella burnetii*, spotted fever group and typhus group *Rickettsiae*, and *Bartonella*
512 *henselae* among volunteer blood donors in Namibia. *PLoS One*. 2014;9(9):e108674.
- 513 27. Lederer S, Lattwein E, Hanke M, Sonnenberg K, Stoecker W, Lundkvist Å, et al. Indirect
514 Immunofluorescence Assay for the Simultaneous Detection of Antibodies against Clinically
515 Important Old and New World Hantaviruses. *Plos Neglected Tropical Diseases*. 2013;7(4).
- 516 28. Nakamura A, Nakajima G, Okuyama R, Kuramochi H, Kondoh Y, Kanemura T, et al.
517 Enhancement of 5-fluorouracil-induced cytotoxicity by leucovorin in 5-fluorouracil-resistant
518 gastric cancer cells with upregulated expression of thymidylate synthase. *Gastric Cancer*.
519 2014;17(1):188-95.
- 520 29. Andersen CB, Holst-Jensen A, Berdal KG, Thorstensen T, Tengs T. Equal performance of
521 TaqMan, MGB, molecular beacon, and SYBR green-based detection assays in detection and
522 quantification of roundup ready soybean. *J Agric Food Chem*. 2006;54(26):9658-63.
- 523 30. China SAotPsRo. Technical specification for quality evaluation of nucleic acid test kit.
524 Standardization Administration of the People's Republic of China. 2013.
- 525 31. R. Neill Carey P, F. Philip Anderson P, Harvey George P, Alfred E. Hartmann M, Verlin K.
526 Janzen M, Anders Kallner M, PhD , et al. <User Verification of Performance for Precision and
527 Trueness;Approved Guideline-Second Edition.pdf>. CLSI. 2006.
- 528 32. Liu XJ, Feng JP, Zhang QH, Guo D, Zhang L, Suo T, et al. Analytical comparisons of
529 SARS-COV-2 detection by qRT-PCR and ddPCR with multiple primer/probe sets. *Emerging*

- 530 Microbes & Infections. 2020;9(1):1175-9.
- 531 33. Zhang S, Wang S, Yin W, Liang M, Li J, Zhang Q, et al. Epidemic characteristics of
532 hemorrhagic fever with renal syndrome in China, 2006-2012. BMC Infect Dis. 2014;14:384.
- 533 34. Jiang W, Wang PZ, Yu HT, Zhang Y, Zhao K, Du H, et al. Development of a SYBR Green
534 I based one-step real-time PCR assay for the detection of Hantaan virus. Journal of Virological
535 Methods. 2014;196:145-51.
- 536 35. Zeng P, Yang Z, Bakkour S, Wang B, Qing S, Wang J, et al. Development and validation
537 of a real-time reverse transcriptase PCR assay for sensitive detection of SFTSV. J Med Virol.
538 2017;89(7):1131-8.
- 539 36. Jalal S, Hwang SY, Kim CM, Kim DM, Yun NR, Seo JW, et al. Comparison of RT-PCR,
540 RT-nested PCRs, and real-time PCR for diagnosis of severe fever with thrombocytopenia
541 syndrome: a prospective study. Sci Rep. 2021;11(1):16764.
- 542 37. Wang XG, Zhang QF, Hao F, Gao XNA, Wu W, Liang MY, et al. Development of a Colloidal
543 Gold Kit for the Diagnosis of Severe Fever with Thrombocytopenia Syndrome Virus Infection.
544 Biomed Research International. 2014;2014.
- 545 38. Zuo LL, Miao J, He DM, Fang ZX, Zhang X, Sun CY, et al. Development and
546 characterization of a digital CRISPR/Cas13a based assay for rapid and sensitive diagnosis of
547 severe fever with thrombocytopenia syndrome virus. Sensors and Actuators B-Chemical.
548 2023;388.
- 549 39. Park BJ, Yoo JR, Heo ST, Kim M, Lee KH, Song YJ. A CRISPR-Cas12a-based diagnostic

550 method for multiple genotypes of severe fever with thrombocytopenia syndrome virus. PLoS

551 Negl Trop Dis. 2022;16(8):e0010666.

552 40. Kim WK, Kim JA, Song DH, Lee D, Kim YC, Lee SY, et al. Phylogeographic analysis of

553 hemorrhagic fever with renal syndrome patients using multiplex PCR-based next generation

554 sequencing. Sci Rep. 2016;6:26017.

555

556

557

558

559

560

561

562

563

564

565

566

567

568 **Supporting information**

569 **S1 Fig. Digital PCR Results of SFGR 10^3 copies/ μ L concentration (a)**The scatter

570 plot of SFGR 10^3 copies/ μ L. 3,262.99 copies/ μ L (b)The scatter plot of SFGR 10^1

571 copies/ μ L. 22.17 copies/ μ L.

572 **S2 Fig. Digital PCR Results of SFTSV 10^3 copies/ μ L concentration** (a)The scatter

573 plot of SFTSV 10^3 copies/ μ L.3,629.44 copies/ μ L (b)The scatter plot of SFTSV 10^1

574 copies/ μ L.21.51 copies/ μ L

575 **S3 Fig. Digital PCR Results of HTNV 10^3 copies/ μ L concentration** (a)The scatter

576 plot of HTNV 10^3 copies/ μ L. 3,530.33 copies/ μ L (b)The scatter plot of HTNV 10^1

577 copies/ μ L. 20.13 copies/ μ L

578 **S1 Table. The Ct value of tempreature optimization.**

579 **S2 Table. The Ct values correspond to the concentrations of SFGR different**

580 **gradient primers and probes.**

581 **S3 Table. The Ct values correspond to the concentrations of SFTSV different**

582 **gradient primers and probes.**

583 **S4 Table. The Ct values correspond to the concentrations of HTNV different**

584 **gradient primers and probes.**

585

586

587

588

589

590

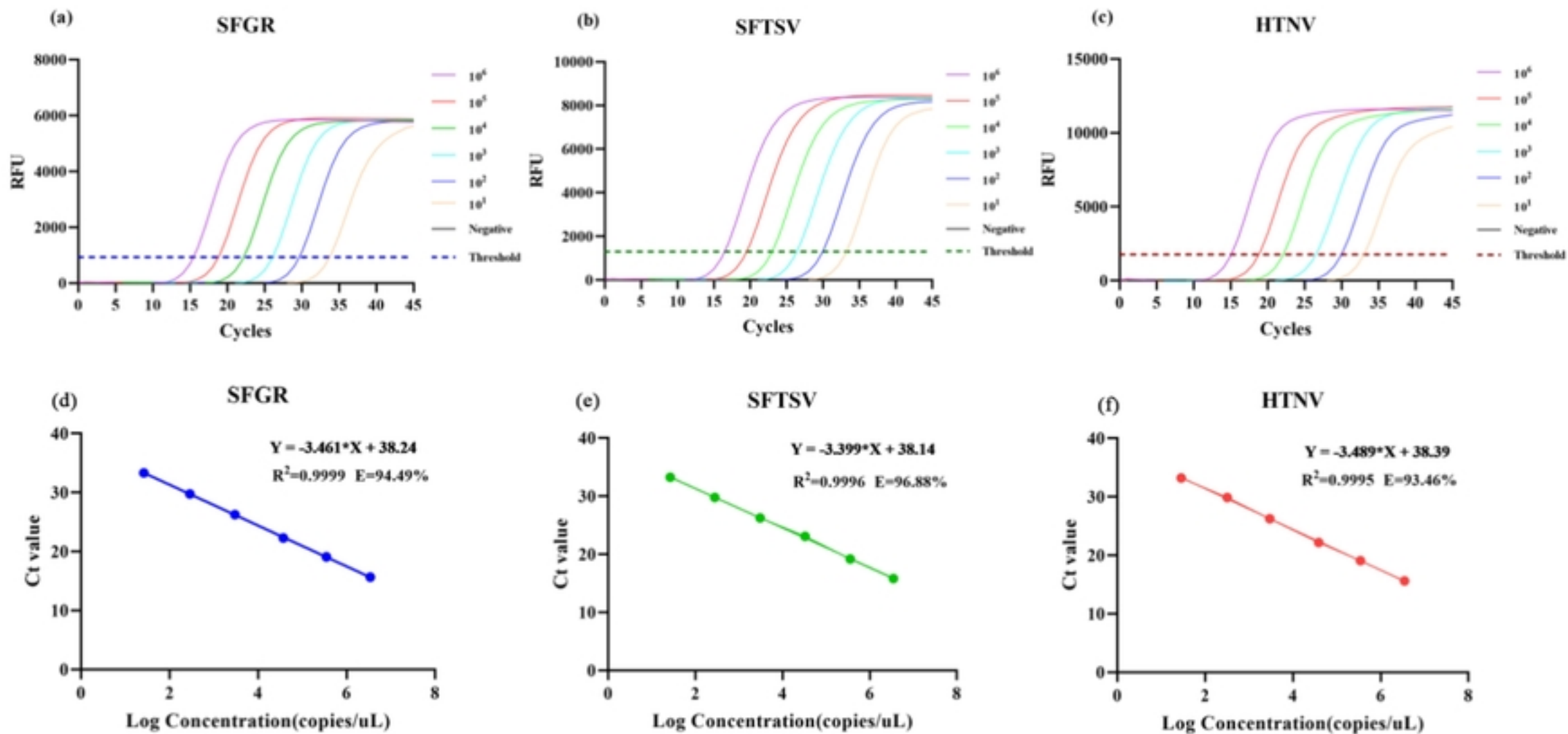


Figure.2

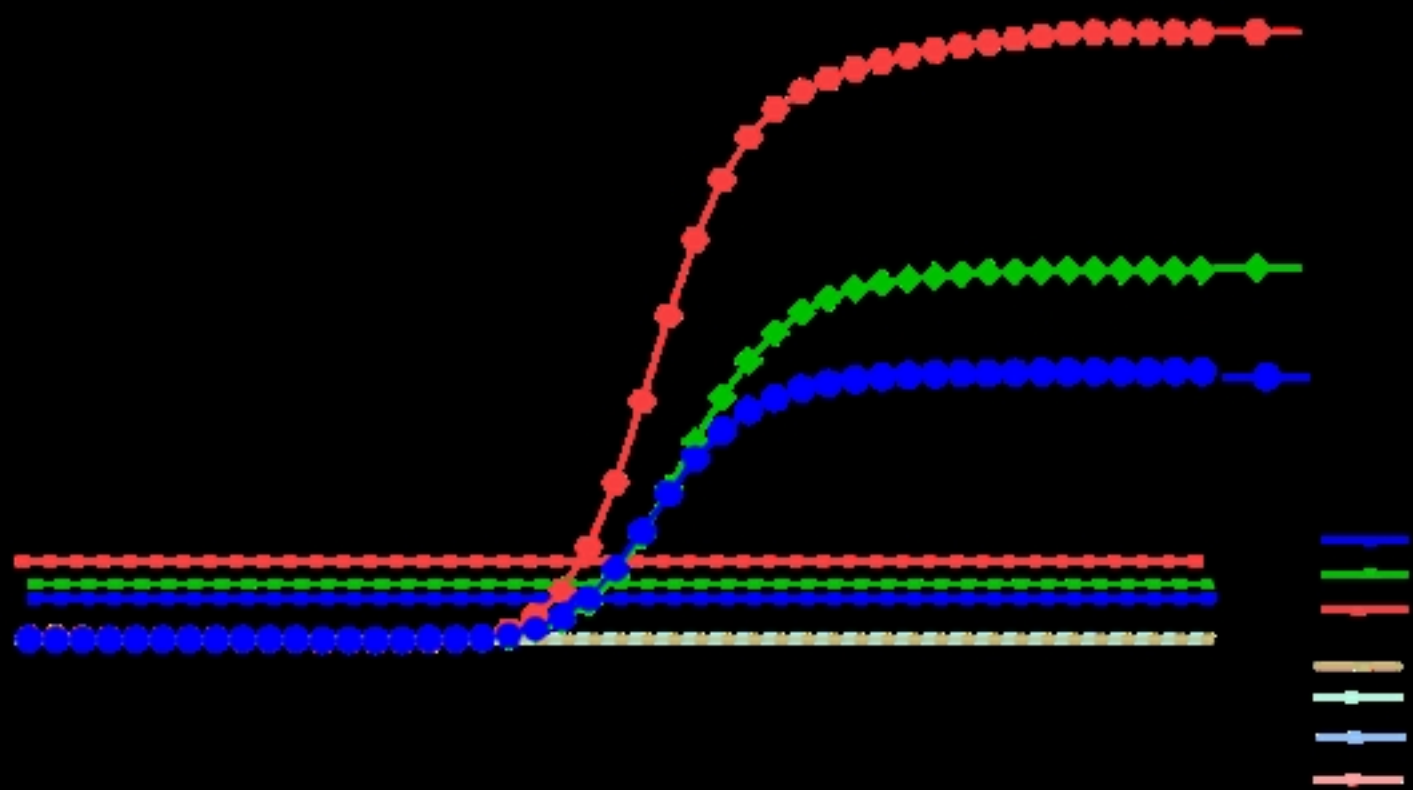
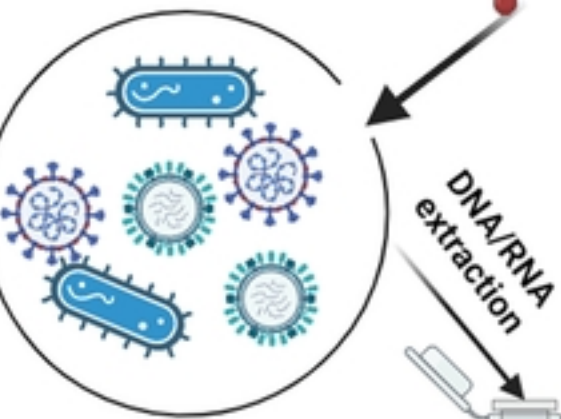
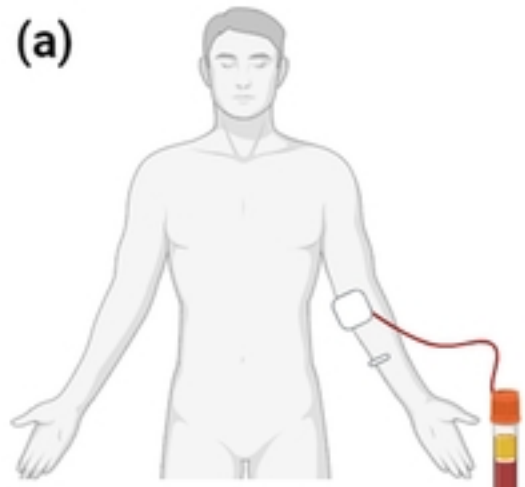
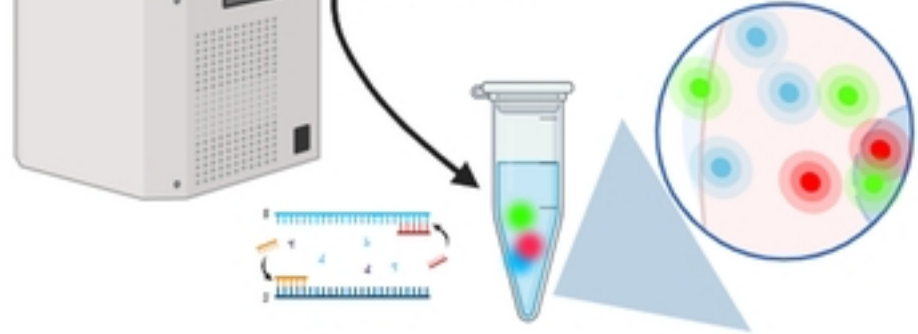


Figure.3

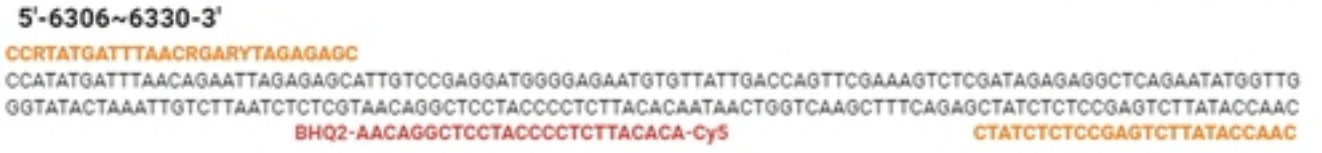
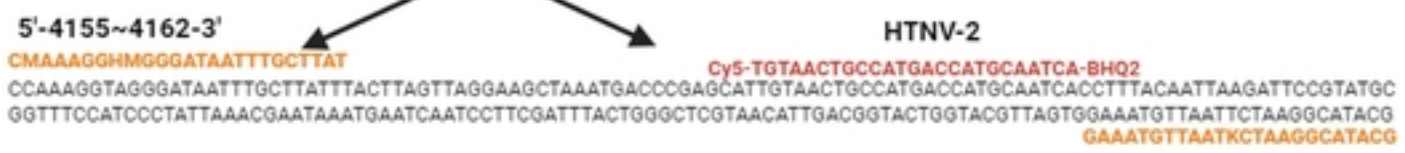
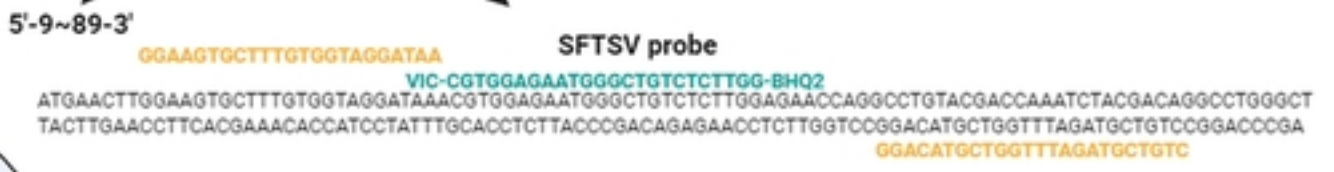
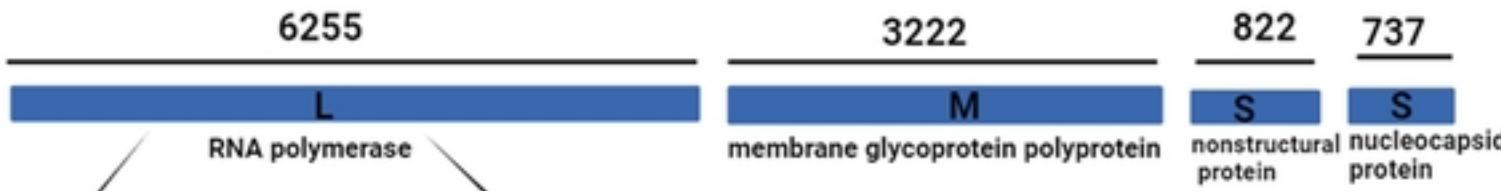
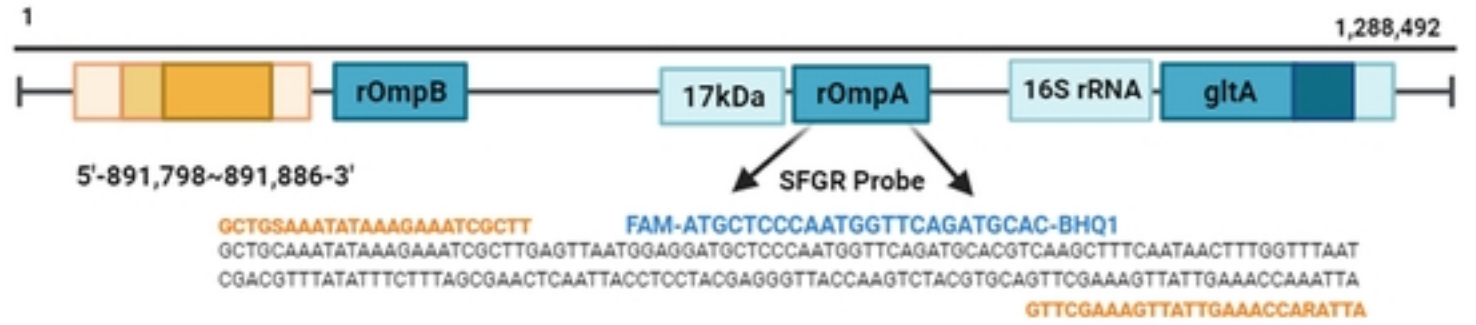
(a)



Reaction



(b)



scheme.1

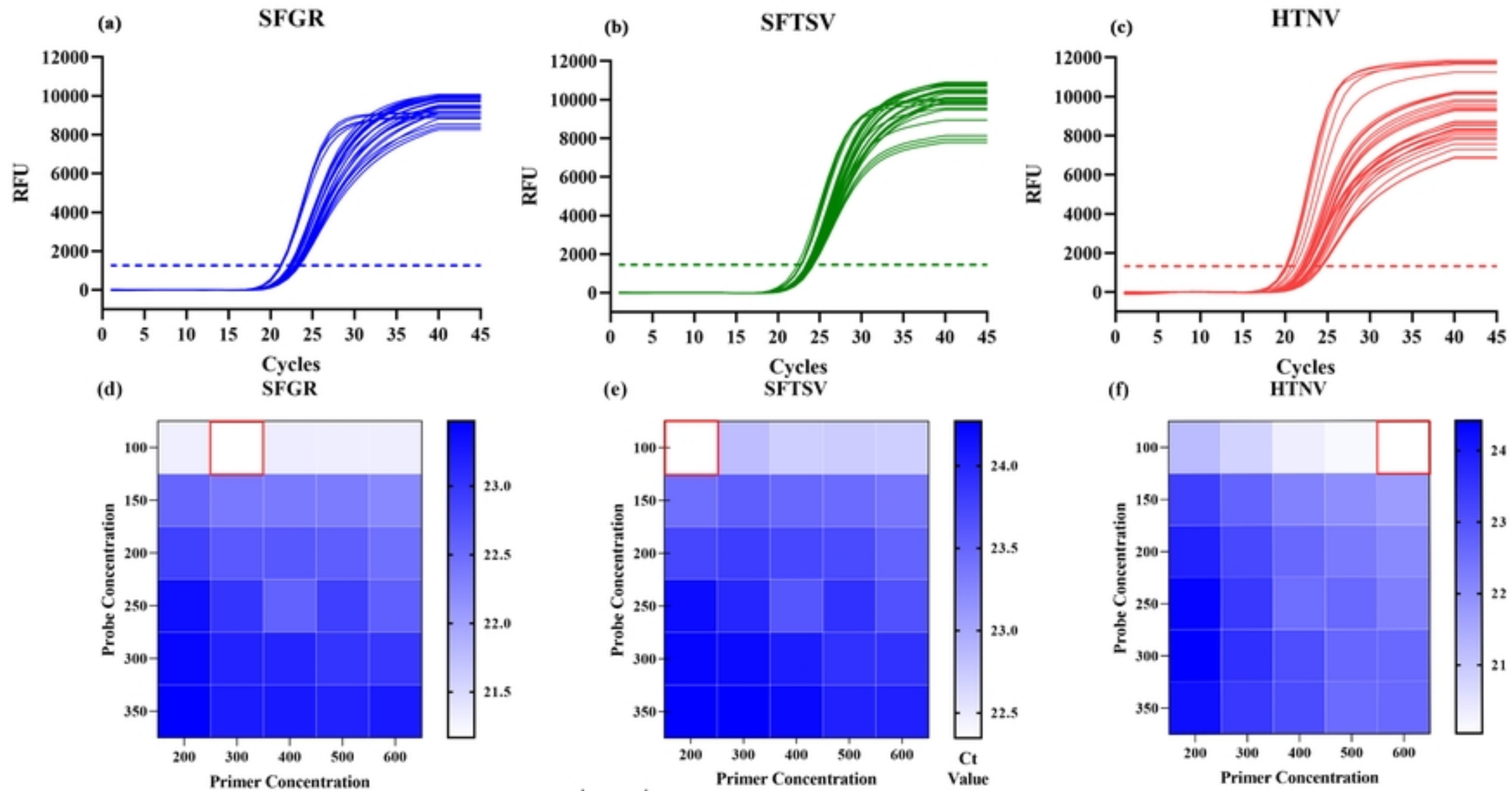


Figure.1